# Thermodynamics of protein denatured states

**Bruce E. Bowler***

**DOI: 10.1039/b611895j**

Recent work on the thermodynamics of protein denatured states is providing insight into the stability of residual structure and the conformational constraints that affect the disordered states of proteins. Current data from native state hydrogen exchange and the pH dependence of protein stability indicate that residual structure can modulate the stability of the denatured state by up to 4 kcal $mol^{-1}$. NMR structural data have emphasized the role of hydrophobic clusters in stabilizing denatured state residual structures, however recent results indicate that electrostatic interactions, both favorable and unfavorable, are also important modulators of the stability of the denatured state. Thermodynamics methods that take advantage of histidine–heme ligation chemistry have also been developed to probe the conformational constraints that act on denatured states. These methods have provided insights into the role of excluded volume, chain stiffness, and loop persistence in modulating the conformational preferences of highly disordered proteins. New insights into protein folding and novel methods to manipulate protein stability are emerging from this work.

## Introduction

The free energy of unfolding a protein, $\Delta G^{\circ}_{u}$, is the difference in the free energy of the native versus the denatured state, $G^{\circ}_{D} - G^{\circ}_{N}$. The overall stability of a protein is also the relatively small difference between large opposing forces,[1] so, even a small number of weak non-covalent interactions in the disordered denatured state of a protein could have an important impact on global stability.

*Department of Chemistry, University of Montana, Missoula, MT 59812, USA. E-mail: bruce.bowler@umontana.edu*

An important focus of this Highlight article will be on recent advances in our ability to assess quantitatively denatured state thermodynamics that are beginning to allow rational manipulation of $\Delta G^{\circ}_{u}$ based on the properties of protein denatured states.

Much work on protein folding and stability has focused on the native state rather than the denatured state. Largely this has been a very fruitful approach because the weak non-covalent interactions that effect protein stability are maximal in the well-ordered compact native states of proteins. Detailed structural data are also available on the native states of many proteins and therefore it is much more straightforward to analyze the contributions of hydrogen bonds, electrostatic interactions, van der Waals interactions and hydrophobic burial to protein stability[2] in the native state versus the structurally ill-defined denatured state. Careful mutational studies coupled to X-ray analysis have demonstrated the importance of native state hydrophobic burial[3,4] and the beneficial impact of optimal native state packing (van der Waals interactions) for protein stability.[5–8] The stabilizing effects of main chain hydrogen bonds,[9] native state salt bridges,[10] particularly when partially buried,[11] and charge/aromatic interactions[12] are also clear. Similarly, relatively simple electrostatic models have been successfully implemented to stabilize proteins by optimizing native state surface electrostatics.[13] Thus, native state analysis has provided a number of useful tools for rational stabilization of a protein through mutagenesis.

The mechanism by which proteins fold from a disordered denatured state to a well-ordered native state is also of fundamental interest. From a practical standpoint, efficient folding provides a primary defense against pathological aggregation of proteins in so-called misfolding diseases.[14] The native state has

**Bruce E. Bowler**

*Bruce E. Bowler grew up in Toronto, Canada. He did undergraduate studies at Brown University, graduating with a BSc in chemistry, magna cum laude, in 1981. He carried out graduate research on platinum antitumor drugs with Stephen J. Lippard at Columbia University, MA, 1982, and MIT, PhD, 1986. Following three years of postdoctoral studies on protein electron transfer reactions with Harry B. Gray and Jack Richards at Caltech, he joined the chemistry faculty at the University of Denver in 1989. In 2006, he moved to the University of Montana as a professor of chemistry and a member of the Center for Biomolecular Structure and Dynamics. His research focuses on denatured and partially unfolded states of proteins and on the effect of protein conformation on biological electron transfer reactions.*

 

provided important clues into the factors which promote fast folding. The topological constraints, or contact-order, of the native fold appear to exercise substantial control over folding rates.[15] Proteins with predominately short-range contacts fold faster than proteins with a prevalence of long-range contacts. Much insight has also been gained into the nature of the transition state for folding, and by extension the mechanism of protein folding, by analyzing the mutual effects on protein stability and folding rates of site-directed mutations based on native state contacts. In this $\phi$-value analysis,[16] mutations which both stabilize the protein and enhance the rate of folding define native state contacts which are also formed in the transition state.

Efficient folding is clearly counter to a random conformational search,[17,18] and whilst a number of means to promote efficient folding have been brought forward,[18–25] a non-random denatured state can also provide for efficient folding. There is substantial evidence from NMR studies that non-random or residual structure exists in denatured states.[26–35] The combination of computational and structural methods has been a particular powerful tool in discerning the nature of this residual structure.[36–39] Fluctuating secondary structure and hydrophobic clusters, both native like and non-native, are evident elements of residual structure. An important observation in the structural[26,32–35] and theoretical work[36–39] is the prominent role of aromatic residues, particularly tryptophan, in stabilizing non-random structure in denatured proteins. Quantifying the impact of residual structure on folding efficiency has been more difficult. A second focus of this Highlight article will be on examples where the recent progress in defining the thermodynamics of denatured states has led to some initial insights into how non-random structure in protein denatured states influences the efficiency of protein folding.

Finally, this Highlight article will discuss novel thermodynamic methods that have been developed to study the formation of the most primitive structure that can form in a disordered protein, a simple loop involving contact between two residues. These studies provide insight into the conformational constraints that operate on a disordered protein. Recent work is also beginning to show that rates of breakage of such primitive loops vary in surprising ways. Understanding the factors that control rates of loop breakage is essential since ultimately efficient folding depends not only on the speed at which simple loops form, but also on their persistence.

## Early history

Interest in protein denatured states has been intense in the last decade.[40] The earliest studies on protein denatured states were carried out in Tanford's laboratory.[41] In a key result, the radius of gyration, as measured by viscosity methods, was found to obey a power law relationship with respect to the number of amino acids in the sequence for proteins dissolved in 5–7.5 M guanidine HCl (gdnHCl).[41,42] The power law exponent, $\nu$, was found to be 0.67, in close accord with the predictions of polymer theories for a random coil with excluded volume ($\nu$ = 0.6 for a good solvent).[43] This power law dependence with $\nu$ = 0.6 has been replicated recently using both NMR[44] and small angle X-ray scattering methods.[45]

A number of results, however, argued against true random coil behavior. Circular dichroism (CD) studies by Tiffany and Krimm[46,47] suggested that denatured proteins had significant contributions from polyproline II structure, a result that has substantial support from recent NMR and CD studies (for reviews see ref. 48,49). Other work from Tanford's lab demonstrated that thermally denatured proteins could be further unfolded by the addition of gdnHCl.[50] Studies on cytochrome *c* in Tsong's lab[51,52] also showed that the compactness of its denatured state depended strongly on pH, the denaturant used and on denaturant concentration. Thus, the notion of a simple random denatured state was questioned early on.

## The modern era of protein denatured state thermodynamics begins

The advent of site-directed mutagenesis methods revolutionized the study of the thermodynamics of protein folding. As discussed above, careful analysis of important interactions in the native state became possible. However, some mutagenesis studies produced results that were difficult to reconcile with effects on native state interactions. In Shortle's lab, studies on Staphylococcal Nuclease (SNase) showed that denaturant *m*-values ($d\Delta G/d[\text{denaturant}]$) could vary dramatically with single-site mutations, both increasing, $m^+$ variants, and decreasing, $m^-$ variants, by up to 50%.[53,54] Since theoretical[55] and empirical[56] studies demonstrate that $m \propto \Delta A$ (the change in solvent-exposed surface area upon unfolding), the degree of unfolding appeared to be changing. While the $m^-$ mutations could be explained by a more labile native state with greater solvent exposure, it was difficult to rationalize the highly compact native state becoming more compact in the $m^+$ variants. Thus, Shortle proposed that these $m^+$ and $m^-$ variants resulted from changes in the degree of residual structure in the denatured state (Fig. 1). A number of spectroscopic studies, including NMR, support these conclusions.[54] Non-additive changes in

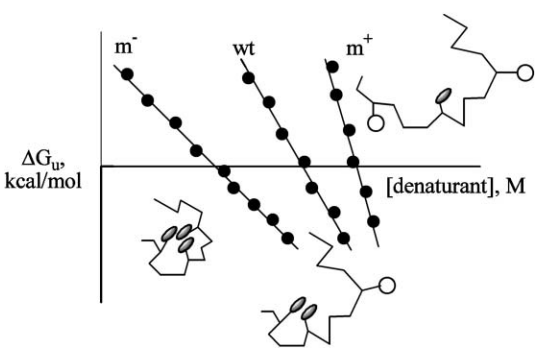


**Fig. 1** $\Delta G_u$ *versus* [denaturant] data (solid circles with lines) for wild type (wt), $m^-$ and $m^+$ variants. Next to each curve are diagrams of how a hydrophobic cluster in the denatured state might respond to mutations leading to changes in compactness.

*m*-values were also observed, which were best interpreted in terms of changes in denatured state structure.[57] To explain changes in *m*-values the denatured state can be viewed as an ensemble of microstates of variable compactness.[53,54] Mutations or variation of the concentration of a denaturing agent can shift the ensemble of microstates to more or less compact structures. This view is supported by the effects of denaturant concentration on denatured state structure as observed by NMR,[30,32] fluorescence energy transfer[58] and hydrodynamic measurements.[59] These data demonstrate that denatured states are more compact and more structured in the absence of denaturant or at lower denaturant concentrations.

Around the same time as Shortle's work, Sauer's laboratory using λ Cro protein,[60] Sturtevant's group using Streptomyces subtilisin inhibitor,[61] and our laboratory using iso-1-cytochrome *c*,[62,63] demonstrated reverse hydrophobic effects on protein stability for mutations at highly solvent exposed sites. In a reverse hydrophobic effect, stability decreases as hydrophobicity increases (Fig. 2), suggesting that an amino acid side chain is more buried in the denatured state than in the native state. In the case of the λ Cro result, later work showed that thermal unfolding of λ Cro can significantly populate a tetrameric intermediate.[64] Such an intermediate could also explain the decreased stability of variants with hydrophobic amino acid substitutions at highly solvent exposed sites in λ Cro. In our iso-1-cytochrome *c* study, however, the *m*-value decreased as hydrophobicity increased providing additional support for a reverse hydrophobic effect.[62,63] Pace's lab also observed a reverse hydrophobic effect when the highly solvent exposed Asp 49 of RNase T1 was replaced with Phe, Tyr or Trp.[65] Decreases in stability on the order of 0.5 to 1.0 kcal $mol^{-1}$ were observed for these charge to hydrophobic mutations. Reverse hydrophobic effects are perhaps not surprising given the denatured state NMR data which demonstrate the presence of persistent hydrophobic clusters in high concentrations of denaturants.[26,32,34] In the case of the denatured state of the drkN SH3 domain, populated in the absence of denaturant, structural data indicate that Trp 32 is more buried than in the native state.[35]

An extreme example of residual structure due to hydrophobic clusters is observed in the case of the α subunit of trytophan synthase.[66,67] The urea dependence of the His 92 NMR resonances give evidence for a persistent hydrophobic cluster, after loss of all secondary structure. It unfolds cooperatively between 5 and 7.5 M urea with an apparent stability of ~8 kcal $mol^{-1}$. Given the stability of the residual structure in this case, this example may best be classified as an intermediate rather than a denatured state.

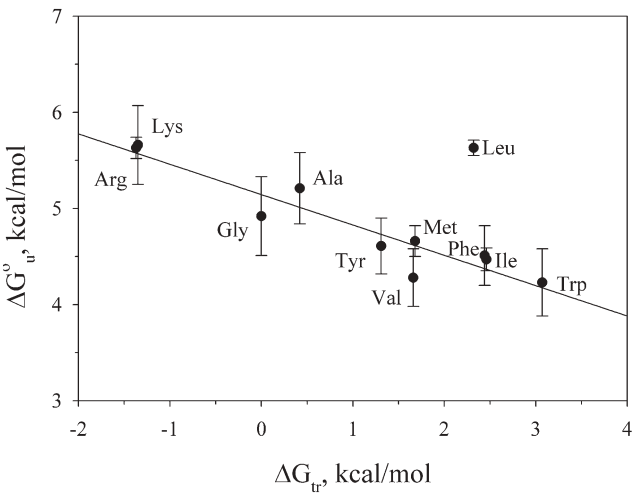


**Fig. 2** Plot of $\Delta G^{\circ}_{u}(H_2O)$ against hydrophobicity of the residue at position 73 of iso-1-cytochrome *c*. The hydrophobicity, $\Delta G_{tr}$, is the free energy of transfer from 1-octanol to water .[140] Error bars are one standard deviation for each $\Delta G^{\circ}_{u}(H_2O)$ value. A linear least-squares fit to the data is shown. The equation of this fit is $\Delta G^{\circ}_{u}(H_2O) = -0.32(\Delta G_{tr}) + 5.14$, $r = 0.94$. Reprinted with permission from L. Herrmann, B. E. Bowler, A. Dong and W. S. Caughey, *Biochemistry*, 1995, **34**, 3040–3047. Copyright 1995 American Chemical Society.

## *m*-Values and $\Delta C_p$

As discussed above, denaturant *m*-values are proportional to the change in solvent-exposed surface area, $\Delta A$, upon unfolding a protein. The heat capacity increment for unfolding a protein, $\Delta C_p$, is usually attributed in a large part to the ordering of water molecules around hydrophobic amino acid side chains exposed to the solvent when a protein unfolds.[1] $\Delta C_p$ is thus expected to be proportional to $\Delta A$ and empirical data demonstrate this propotionality.[56] Due to the proportionality to $\Delta A$, both these thermodynamic parameters have been widely used to detect residual structure in protein denatured states. Although, care must be taken in interpreting denaturant *m*-values since decreases in *m*-values can also be caused by mutations which lead to population of folding intermediates.[68,69]

Disulfide bonds introduce constraints into the denatured state of a protein. In the case of RNase T1, as the number of disulfide bonds decreases the *m*-value increases, consistent with greater solvent exposure in the denatured state.[70] Similarly, a long-range disulfide bond engineered between residues 20 and 102 in iso-1-cytochrome *c* led to a more compact denatured state as indicated by $\Delta C_p$ and *m*-values which decreased by a factor of ~2 relative to the wild type protein.[71] The observed decrease in stability for this iso-1-cytochrome *c* variant, which runs counter to the expected destabilization of the denatured state by this long range disulfide cross-link, is consistent with the stabilization of the compact denatured state by residual structure. Recently, our laboratory has shown that denaturant *m*-values decrease as the size of a histidine–heme loop in the denatured state of iso-1-cytochrome *c* increases.[72] This result demonstrates that as more of the protein sequence is constrained into a loop the denatured state becomes progressively less solvent-exposed.

Despite the very consistent effects of denatured state constraints on *m*-values

 

in the above work, structural correlates of denatured state compactness with changes in *m*-values are not always straightforward. Bolen's lab found no correlation of the rank order of *m*-values of SNase variants with their Stoke's radii as determined by size exclusion chromatography.[73] While CD data consistent with loss of denatured state structure in $m^+$ variants of SNase is common,[74,75] obtaining similar data for $m^-$ variants has been more elusive.[75] More recently, hydrogen exchange data have shown that the β-barrel of SNase is more stable in $m^-$ than in $m^+$ variants, suggesting that mutation-induced changes in residual structure are localized in this portion of SNase.[75]

Recent work comparing mesophilic and thermophilic RNase H indicates that residual structure in the denatured state provides one mechanism to enhance stability of proteins at higher temperature. A smaller $\Delta C_p$ causes the temperature dependence of $\Delta G$ to be more shallow leading to significantly higher midpoint temperatures, $T_m$, for unfolding (eqn. (1), where $\Delta H^\circ$ is the enthalpy of unfolding at $T_m$). The $\Delta C_p$ for unfolding of the thermophilic RNase H is $\sim$1.8 kcal mol$^{-1}$ K$^{-1}$ compared to $\sim$2.7 kcal mol$^{-1}$ K$^{-1}$ for mesophilic RNase H and studies with chimeric proteins demonstrate that the stable core of the protein is responsible for this difference.[76] Furthermore, careful calorimetric studies show that at low pH the heat capacity of the denatured state of thermophilic RNase H is $\sim$0.8 kcal mol$^{-1}$ K$^{-1}$ lower than the heat capacity of the denatured state of mesophilic RNase H consistent with a more compact denatured state with residual structure.[77] Equally interesting is the observation that the heat capacity of the denatured state of thermophilic RNase H decreases abruptly at pH 3.8. This result is consistent with protonation of carboxylic acid side chains promoting formation of hydrophobic clusters in the denatured state of the protein. Finally, mutagenesis methods show that mutations that break up the hydrophobic clusters in the denatured state of thermophilic RNase H increase the $\Delta C_p$ of the protein.[78]

$$\Delta G^\circ_u(T) = \Delta H^\circ - T(\Delta H^\circ/T_m) + \Delta C_p\{T - T_m - T\ln(T/T_m)\} \quad (1)$$

## Assessing the stability of residual structure by hydrogen exchange

While data showing reverse hydrophobic effects and changes in *m*-values and $\Delta C_p$ are important indicators of residual structure, more direct measurements on the thermodynamics of the denatured state are desirable. Hydrogen exchange (HX) has been useful in studying the order of formation and the relative stability of protein folding intermediates.[21,79] In principle, the degree of protection of amide NH groups from exchange provides a direct measure of the stability of residual structure in a denatured protein. To date, however, the number of successful applications of this method to a denatured protein has been small. Typically, gdnHCl or urea is used to denature proteins and these agents disrupt residual structure in denatured proteins.[30,32,58,59,80] In one successful case, the acid denatured state of horse cytochrome *c* under low salt conditions (0.02 M, *i.e.* not the molten globule state) was shown to retain protected structure in the N- and C-terminal helices and in the 60's helix.[81] The stability of all helices was $\sim$1 kcal mol$^{-1}$ ($K_{eq} \sim 10$). Isolated peptides based on these 3 helices have little to no helical structure suggesting that the residual structure in the acid denatured state is promoted by some sort of loose tertiary interaction.

In native state HX, the rate of exchange of amide NH groups is measured under native conditions:[79]

$$\text{Closed} \underset{k_{cl}}{\overset{k_{op}}{\rightleftharpoons}} \text{Open} \xrightarrow{k_{int}} \text{Exchanged}$$

Typically, under native conditions, $k_{cl} >> k_{int}$ (EX2 conditions) and $k_{obs} = K_{op}k_{int}$, where $K_{op}$ ($k_{op}/k_{cl}$) is the equilibrium constant for unfolding the structure which protects the amide NH from exchange and $k_{int}$ is the intrinsic rate of exchange for that amide NH in an unstructured peptide. Thus, in principle, $\Delta G^\circ_u$ can be evaluated from $\Delta G_{HX} = -RT\ln(k_{obs}/k_{int})$. Initial work on a number of proteins demonstrated that many proteins had amide NH residues that yielded $\Delta G_{HX}$ which was significantly larger than $\Delta G^\circ_u$ measured using standard spectroscopic probes (CD, fluorescence).[82–84] These superprotected residues could define regions of residual structure in the denatured state. However, the majority of these early instances of superprotection could be explained when the effects of proline isomerization were taken into account (Since closing is typically faster than the rate of proline isomerization, the denatured state probed by HX has X–Pro peptide bonds with the native conformation and thus will be higher in energy than the unfolding to a denatured state with equilibrated X–Pro peptide bonds).[85] Increasingly, additional instances of proteins showing HX superprotection that defy explanation by proline isomerization, deviations from EX2 behavior,[83] or errors in $k_{int}$, have emerged in the last few years. These include two different SH3 domains,[86,87] SNase,[75] the prion protein from Syrian Hamster (Fig. 3),[88] thioredoxin[89] and the Src SH2 domain.[80] The superprotection in these cases ranges from 0.5–2.0 kcal mol$^{-1}$, consistent with modest to significantly stable residual structure in the denatured states of these proteins. For SNase[75] and thioredoxin,[89] superprotection is localized in the β-structure rather than in the helices. In cases where superprotection is found in both helical and β-sheet regions, the proteins are predominately β-sheet proteins.[80,86] This observation suggests that β-structure may have a greater tendency to form residual structure under native conditions, and is not surprising given the greater per residue hydrophobic burial required for two layers of β-sheet *versus* two interacting helices.

Not all *bone fide* HX superprotection has been interpreted in terms of residual structure in the denatured state. The HPr protein from *Bacillus subtilis* shows extensive superprotection with $\Delta G_{HX}$ values up to $\sim$2 kcal mol$^{-1}$ greater than $\Delta G^\circ_u$ measured using CD as a probe.[90] In this case, kinetic data clearly demonstrate the presence of a burst phase intermediate that accounts for the additional 2 kcal mol$^{-1}$ of stability. Distinguishing between a high energy intermediate and residual structure in the unfolded state will always involve subtle distinctions. However, it is clear from the available HX data that an increasing number of proteins have residual structure in their unfolded states under native conditions. This residual structure will thus be important in

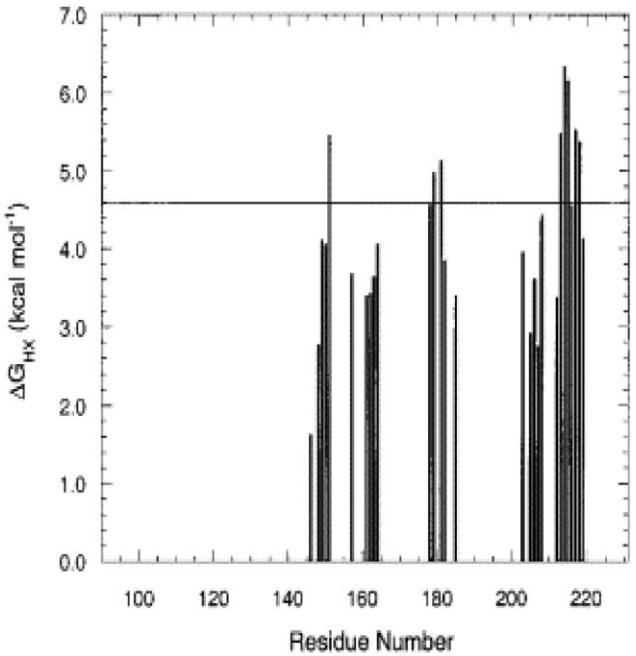


**Fig. 3** HX superprotection in the Syrian Hamster prion protein. Free energy determined from HX protection factors ($\Delta G_{HX}$) for Syrian Hamster prion protein (PrP) is shown as a function of residue number. The continuous horizontal line denotes the global stability, $\Delta G_u^\circ$, of PrP monitored by CD. No protection is observed in the N-terminal region of PrP. Most protected residues lie in the three helices of PrP. Many of these residues show substantial superprotection. Reprinted from N. M. Nicholson, H. Mo, S. B. Prusiner, F. E. Cohen and S. Marqusee, *J. Mol. Biol.*, 2002, **316**, 807–815, Copyright 2002, with permission from Elsevier.

directing folding of these proteins under cellular conditions and can potentially be used to manipulate global stability.

## Ionic interactions in protein denatured states

The stability of most proteins is pH dependent. The pH dependence of stability is caused by the differences in the p$K_a$ value for an ionizable group in the native *versus* the denatured state. This linkage of stability to pH can be represented by a thermodynamic cycle (Fig. 4).

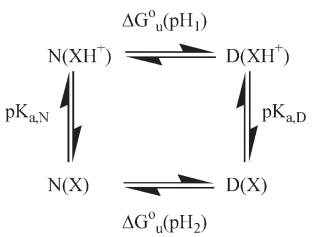


**Fig. 4** Thermodynamic cycle showing the linkage between protein stability and ionization state for a protein with a single ionizable group with a p$K_a$ that is different in the native and the denatured state of the protein.

Evidence for electrostatic interactions in the denatured state comes from several experimental avenues. Studies on the effects of surface electrostatics on protein stability using RNase T1, RNase A and T4 lysozyme have shown that mutations predicted to increase stability based on Coulombic interactions in the native state often cause much less stabilization than expected. These data have been interpreted in terms of stabilizing electrostatic interactions in compact denatured states.[65,91] The observed deviations from stability enhancements predicted by native state electrostatics suggest that electrostatic interactions can stabilize the denatured state by 1 to 4 kcal mol$^{-1}$. Denatured states are expected to be more susceptible to Debye–Hückel screening and thus variants where denatured state electrostatics are a particularly important factor should be strongly stabilized by increased ionic strength, as is observed.[91] Another observation demonstrating the importance of electrostatic interactions in the denatured state is that denaturant *m*-values are affected by pH.[92–95] In particular, *m*-values for many proteins increase at low pH as the net positive charge on a protein increases.

The evidence that electrostatic interactions are significant in the denatured state provides another means of quantitatively assessing the contribution of the denatured state to the overall stability of a protein. The change in stability as a function of pH can be expressed in terms of the linkage relationship in eqn (2), where $\Delta Q$ is the difference in the number of protonated groups

$$\frac{\partial \Delta G^o}{\partial pH} = 2.303 RT \Delta Q \qquad (2)$$

in the denatured *versus* the native state ($Q_D - Q_N$).[41] Using the integrated form of eqn (2), the effects of pH on stability can be assessed relative to some reference pH, $pH_{ref}$, if the p$K_a$ values of all ionizable groups are known in the native and denatured state:

$$\Delta\Delta G^o(pH - pH_{ref}) = RT \sum_{i=1}^{j} \ln \left[ \frac{\left(1 + 10^{(pH - pK_{i,N})}\right)\left(1 + 10^{(pH_{ref} - pK_{i,D})}\right)}{\left(1 + 10^{(pH_{ref} - pK_{i,N})}\right)\left(1 + 10^{(pH - pK_{i,D})}\right)} \right] \qquad (3)$$

where $pK_{i,N}$ and $pK_{i,D}$ are the p$K_a$s of the $i^{th}$ ionizable group in the native and denatured state, respectively.[96] The p$K_a$s of the ionizable groups in the native state can be measured directly by NMR methods. Typically, model compound data are used for the p$K_a$s of ionizable groups in the denatured state. Studies with peptides, however, have shown that local sequence can significantly perturb the p$K_a$s of ionizable groups in disordered peptides demonstrating that isolated amino acid model compounds do not always provide the best denatured state p$K_a$s.[96]

Eqn (2) and eqn (3), when applied to the pH dependence of stability of the N-terminal domain of ribosomal protein L9 (NTL9),[96–98] barnase,[99,100] CI2,[101] SNase,[94] and turkey ovomuciod third domain[102] have demonstrated significant deviations of denatured state p$K_a$ values from model compound or peptide p$K_a$ values. For barnase and CI2, the p$K_a$s of acidic residues in the denatured state are, on average, 0.3 to 0.4 units lower than those of model compounds. Similarly, depressed p$K_a$s for histidines in the denatured state must be invoked to explain the $\sim$4 kcal mol$^{-1}$ discrepancy in the pH dependence of the stability of SNase measured by denaturant or

 

temperature unfolding above pH 5 relative to that predicted from potentiometric titration under native conditions *versus* in 6 M gdnHCl. Electrostatic interactions in the denatured states of these proteins are clearly significant, proving that hydrophobicity is not the only source of denatured state compactness.

Denatured state electrostatic interactions are not always observed. For example, the pH dependence of the stability of the C-terminal domain of ribosomal protein L9 (CTL9) shows no significant deviation from that predicted using model compound p$K_a$s for the histidines of denatured CTL9.[103] Similarly, for a number of proteins, mutation-induced changes in stability are well-predicted based solely on native state electrostatics.[13]

Site-directed mutagenesis and NMR methods have been successful in determining specific residues involved in electrostatic interactions in protein denatured states. Of the many acidic and basic residues in NTL9 (Fig. 5A), the interaction between Lys 12 and Asp 8 was found to account for 1.2 of the 1.8 kcal mol$^{-1}$ electrostatic stabilization of the denatured state (Fig. 5B) by mutating these residues to non-ionizable amino acids.[97,98] Interestingly, a disordered peptide incorporating these two residues does not provide evidence of electrostatic interaction between Lys 12 and Asp 8. This observation suggests that long-range, presumably hydrophobic interactions, hold these residues in close enough proximity in the denatured state to produce electrostatic stabilization. Comparison of $\Delta Q$ extracted from the pH dependence of stability of wild type and mutant proteins can also be used to estimate p$K_a$s of a side chain in the native *versus* the denatured state. For example, calculation of $\Delta\Delta Q$ for wild type CI2 relative to an Asp 52→Asn variant provided p$K_a$ values of 2.5 and 3.8 for the Asp 52 in the native and denatured states, respectively.[101] A recently developed NMR pulse sequence has allowed determination of the p$K_a$s of all the acidic residues in the denatured state of the drkN SH3 domain.[104] In this instance, no general decrease in p$K_a$ values for Asp and Glu sides chains in the denatured state is observed.[105] Unlike NTL9, the p$K_a$s that do shift appear to

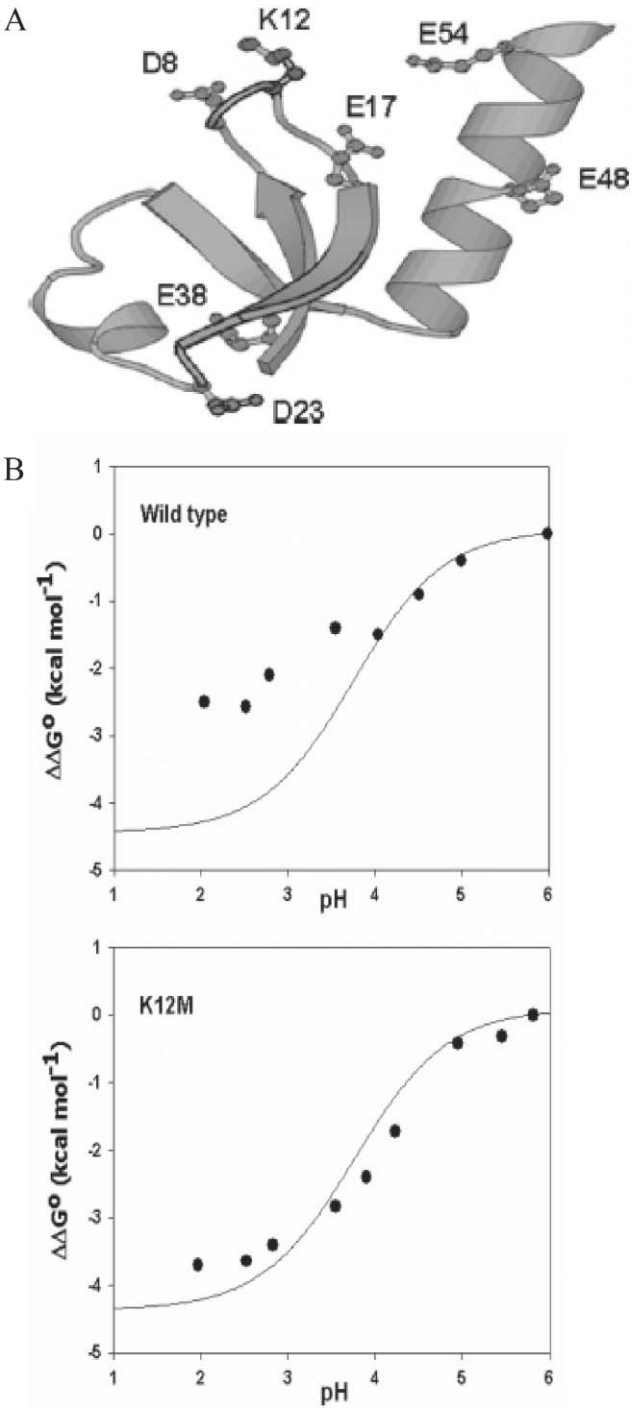


**Fig. 5** (A) Ribbon diagram of NTL9 showing the side chain of Lys 12 and of all acidic residues. (B) The change in $\Delta G_u^\circ$, $\Delta\Delta G^\circ$, as a function of pH for wild type NTL9 and its K12M variant. $\Delta\Delta G^\circ$ is referenced to pH 6. The solid curve represents the predicted change in stability using eqn (3), the p$K_{i,D}$ measured using peptides corresponding to various segments of NTL9 and the p$K_{i,N}$ measured directly for the native state using NMR. A strong deviation from the predicted curve is observed for wild type NTL9 consistent with a stabilizing electrostatic interaction in the denatured state. The data for the K12M variant correspond much more closely to the predicted pH dependence of $\Delta\Delta G^\circ$ indicating that Lys 12 is an important contributor to stabilization of the denatured state of NTL9 *via* favorable electrostatic interactions. Parts A and B are reprinted with permission from J.-H. Cho, S. Sato and D. P. Raleigh, *J. Mol. Biol.*, 2004, **338**, 827–837, Copyright 2004, with permission from Elsevier.

be attributable to local rather than long-range denatured state interactions.

In summary, electrostatic effects can be important in modulating the stability of the denatured state. Such electrostatic interactions can affect protein stability by up to 4 kcal $mol^{-1}$. Thus, engineering denatured state electrostatics can be an excellent strategy for manipulating $\Delta G_u^\circ$. It is also evident that the nature and strength of denatured state electrostatic interactions vary from one protein to another. Therefore, while an important addition to the toolbox of methods for modulating protein stability, the efficacy of manipulating denatured state electrostatics will vary from protein to protein.

## Thermodynamics of denatured state loop formation

The most primitive contact that can be made by a disordered protein is a simple loop. The conformational constraints that mediate loop formation are important because they control the efficiency of folding and thus can provide insight into the basis of misfolding diseases.[14] A number of elegant methods have been developed to study the kinetics of loop formation and these studies have been used to define a speed limit for folding (for recent reviews see ref. 106–108). Kinetic methods provide important insight into how fast a simple loop forms while equilibrium methods provide complementary insight into loop persistence. In this Highlight article, I focus on equilibrium methods of measuring loop formation, developed in this laboratory.

The methods worked out in this laboratory exploit iron–heme coordination chemistry. Variants of yeast iso-1-cytochrome *c* are produced that have only one histidine besides the native state heme ligand, His 18. Under denaturing conditions, loops are formed when the unique histidine binds to the sixth coordination site of the heme. The stability of the loop can be measured by a simple pH titration (Fig. 6). The loop size formed under denaturing conditions is controlled by varying the sequence position of the engineered histidine. Factors such as chain stiffness and how closely the chain represents a random coil can be evaluated from the dependence of loop stability on loop size. For example, the scaling exponent, $v_3$, for loop probability as a function of the logarithm of loop size, log(*n*), can be determined and compared to values expected for a random coil.

Initial work showed that a loop of 37 residues (histidine at position 54) was more stable in 3 M gdnHCl than shorter loops of 9 and 16 residues providing initial evidence for a significant deviation from random coil behavior in the denatured state of iso-1-cytochrome *c*.[109,110] A more complete length dependence of denatured state loop formation in 3 M gdnHCl encompassing eight loop sizes ranges from 9 to 83 amino acids in length demonstrated that the 37 residue loop was the most stable loop (Fig. 7A).[111] Fluorescence energy transfer methods applied to denatured iso-1-cytochrome *c* show that the polypeptide chain near His 54 favors structures where the heme is nearby,[58] consistent with the observed stability of this particular loop. The lower stability of shorter loops was attributable to chain stiffness. For longer loops, a scaling exponent of approximately −4.0 was observed, well out-of-line with the value of −1.5 expected for a freely jointed random coil[112,113] or the range −1.8 to −2.4 predicted for a random coil with excluded volume.[112–114] We attributed this deviation to residual structure in the loops. Large scaling exponents have also been observed for DNA loop formation and were attributed to hydrophobic interactions in smaller loops.[115,116] Studies on the gdnHCl dependence of denatured state loop stability[117] using our iso-1-cytochrome *c*system, produced *m*-values that decreased from 0.45 kcal $mol^{-1}$ $M^{-1}$to 0.15 kcal $mol^{-1}$ $M^{-1}$ as the loop size increased from 37 to 83, suggesting that residual structure increased as loop size decreased (Fig. 7A). The scaling exponent, $v_3$, also decreased to values near −2.0 in 5 and 6 M gdnHCl, consistent with values expected for a random coil with excluded volume, as might be expected under strong denaturing conditions (Fig. 7A).

To investigate the possibility that residual structure is promoted by loop formation, we measured the kinetics of denatured state histidine–heme loop formation and breakage.[118] In 3 M gdnHCl,

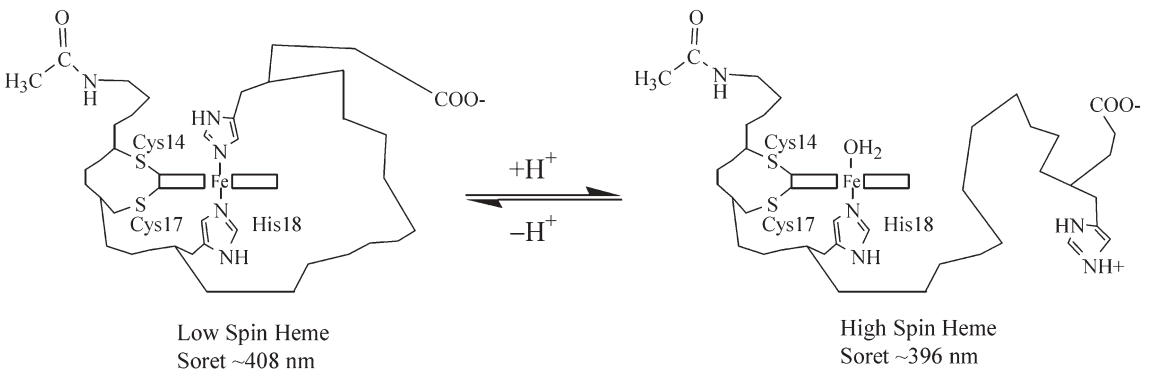


**Fig. 6** Schematic representation of the histidine–heme loop formation equilibrium in the denatured state of iso-1-cytochrome *c*. This scheme has been used to measure the stability of denatured state loops as a function of loop size. The iso-1-cytochrome *c* variants all contain mutations that lead to acetylation of the N-terminus during expression preventing interference from N-terminal amino group–heme binding. At high pH, the single engineered histidine binds to the sixth coordination site of the heme forming a loop. As pH is lowered, the histidine–heme loop breaks giving an apparent $pK_a$, $pK_a$(obs), for this process. $pK_a$(obs) = $pK_{loop}$ + $pK_a$(His), where $pK_{loop}$ is the stability of the loop when the histidine is fully deprotonated and $pK_a$(His) is the $pK_a$ of the histidine.

 

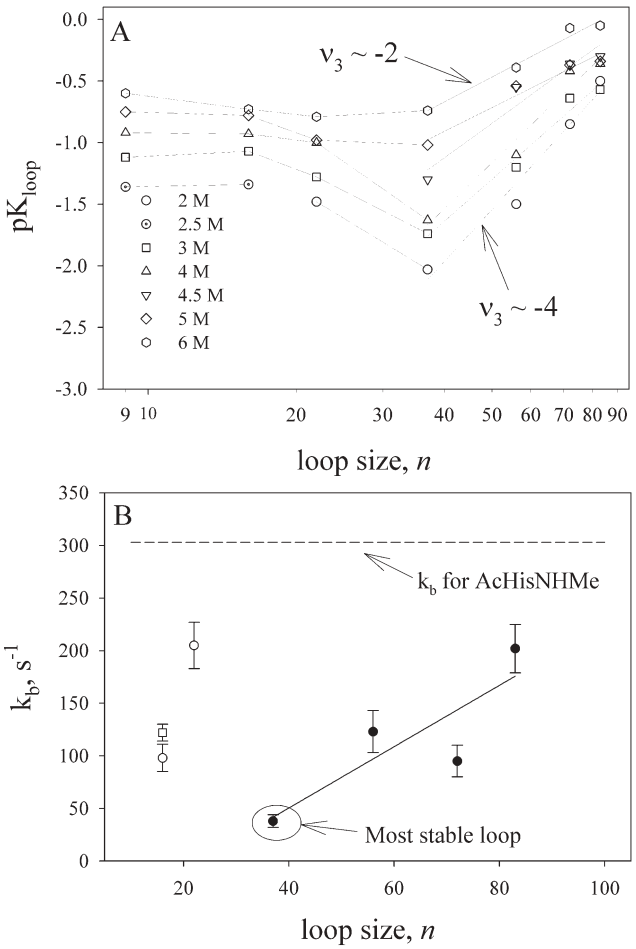


**Fig. 7** (A) The stability of denatured state loop formation, $pK_{loop}$, as a function of loop size (logarithmic scale) and [gdnHCl]. The most stable loop is 37 residues in length (His 54); its stability is also the most sensitive to [gdnHCl]. The scaling exponent, $\nu_3$, varies with [gdnHCl] from a maximum of $\sim -4$ at 2 M gdnHCl to a minimum of $\sim -2$ at 6 M gdnHCl. $pK_{loop}$ levels off for loop sizes less than $\sim 20$ amino acids due to chain stiffness. Reprinted from E. Wandschneider and B. E. Bowler, *J. Mol. Biol.*, 2004, **339**, 185–197, Copyright 2004, with permission from Elsevier. (B) The rates of loop breakage, $k_b$, as a function of loop size in 3 M gdnHCl. For all loop sizes, $k_b$ is less than $k_b$ for *N*-acetylhistidine-*N*-methylamide (AcHisNHMe). The most stable 37 residue loop (His 54) has the slowest rate of loop breakage, 10-fold slower than for AcHisNHMe. The open square data point for the 16 residue loop size is for a loop formed with a histidine on the N-terminal side of the heme. All other data points are for histidines on the C-terminal side of the heme.

the scaling exponent for the rate of loop formation decreased to $-1.8$ (relative to $\sim -4.0$ under equilibrium conditions) indicating that the deviation from random coil behavior could be attributed to the closed loop form. Indeed rates of loop breakage varied considerably, although irregularly with loop size and were all less than the rate of breakage of the bond between the heme of denatured iso-1-cytochrome *c* and exogenously added *N*-acetylhistidine-*N*-methylamide (Fig. 7B). Although the variation of rates of loop breakage may be due in part to residual structure, given the irregular dependence of the rate of loop breakage on loop size, the variation in loop breakage rates may be attributable more broadly to the "internal friction" of the polypeptide chain, which includes such factors as rotational barriers, as well as side chain interactions.[119] Studies on the denaturant dependence of loop breakage should provide some insight into the factors controlling denatured state loop breakage rates.

We have also been able to investigate excluded volume effects on denatured state loop formation using our histidine–heme loop formation methods. Since heme is attached asymmetrically to *c*-type cytochromes, the steric constraints on denatured state loop formation differ dramatically for histidines on the N- *versus* the C-terminal side of the heme. For histidines on the C-terminal side of the heme the protein chain has to wrap around the heme for the histidine to bind to the heme (Fig. 6). Thus, the heme creates a local excluded volume effect that biases the conformational distribution of the protein chain toward the His 18 side of the heme. We find, that for loops of similar sizes, the stability of denatured state histidine–heme loops is $\sim$10-fold higher for loops formed from the N- *versus* the C-terminal side of the heme.[120] Thus, local excluded volume effects can have an important impact on which contacts are likely to form in the early stages of folding.

Thermodynamic methods for measuring denatured state loop formation have provided significant new insights into the conformational constraints that act on disordered proteins. In particular, while kinetic methods show that smaller loops form faster,[106–108] our equilibrium approach demonstrates that the smallest loops are not always the most stable ones and thus not necessarily the ones that will lead to productive folding. Given that expanded and compact forms of the denatured state appear to be in rapid equilibrium on the time scale of folding,[121–123] the thermodynamic stability or persistence of simple loops is expected to be an important factor in guiding the folding process. Similarly, our methods have shown that local excluded volume effects can modulate contact probabilities by a factor of 10. Thus, as structure begins to form excluded volume becomes an important mediator of the folding pathway.

## Denatured state stability and folding rates

The careful characterization of denatured state thermodynamics in a number of systems has made it possible to determine the degree to which residual structure affects the rate of folding of a protein. Heme misligation by histidine[124–129] or the N-terminal amino group[128,129] in the denatured state is one well-characterized example which slows the rate of folding of cytochrome

*c*. The slowing of folding is consistent with a rapid pre-equilibrium, involving histidine *versus* water in the sixth coordination site of the heme, occurring in advance of productive folding *via* the native Met 80-heme ligation.[125] Folding is slowed more when multiple non-native ligands compete for heme ligation in the denatured state,[128] or when a histidine with a particularly strong affinity for the heme is present.[129]

In the case of NTL9 and ribonuclease Sa, the well-understood electrostatic stabilization of the denatured state has allowed the effect of these interactions on folding kinetics to be directly measured. In both cases, the electrostatic interactions in the denatured state are non-native. Thus, if the non-native interactions persist in the transition state, then mutations which remove the denatured state electrostatic interaction will not affect the folding rate. However, unfolding will be affected since both the transition state and the denatured state will be stabilized or destabilized relative to the native state (Fig. 8A). For both NTL9[97] and ribonuclease Sa,[130] minimal change in the folding rate is observed for mutations which modulate denatured state electrostatic interactions. The mutations strongly affect the unfolding rate for both proteins. The simplest explanation for this observation is that the non-native denatured state interactions persist in the transition state (Fig. 8B).

Models such as the Diffusion–Collision model,[131] predict that residual denatured state structure will speed folding. Recent studies on the villin headpiece subdomain indicate that significant residual structure is retained in the first two helices of the domain and is centered around a cluster of phenylalanines that form the hydrophobic core of the folded protein.[132] Conversion of phenylalanines 47 and 51 to leucine significantly reduces the residual structure in a peptide model of the first two helices. The effect of the F47L/F51L double mutant of the villin headpiece subdomain was tested to see if loss of residual structure slowed folding.[133] Surprisingly, the folding rates of the native and double mutant proteins were nearly identical. The result suggests that for some proteins the denatured state may be a complex mix of native and non-native interactions. In the case of the villin headpiece subdomain, a decrease in

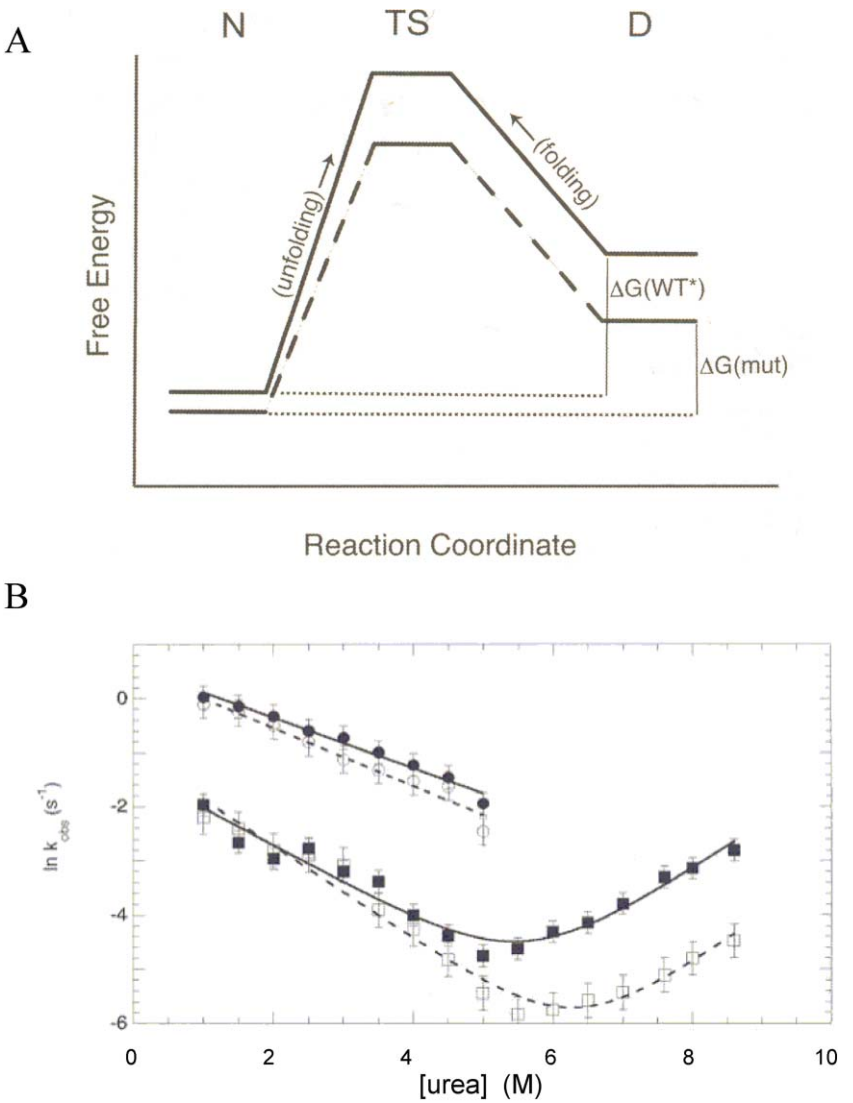


**Fig. 8** (A) Schematic diagram of the effect of non-native electrostatic interactions on the relative energies of the Native state (N), Transition State (TS) and Denatured state (D) of a protein. In this case the electrostatic interaction is formed in both the D and TS states of the protein and is unfavorable in the wild type (WT) protein. Removal of the electrostatic interaction in the mutant (mut) protein lowers the energies of both the TS and the D states by the same amount causing unfolding to be faster but leaving the rate of folding unchanged. (B) Folding and unfolding rates for fast and slow phases of ribonuclease Sa as a function of [urea]. The folding rate is unchanged for the wild type (fast phase, open circle; slow phase, open square) and mutant (D17R) which relieves the denatured state charge repulsion (fast phase, closed circle; slow phase, closed square). The unfolding rate is much faster for the mutant protein than the wild type consistent with the scheme in part A. Parts A and B are reprinted with permission from J. M. Trefethen, C. N. Pace, J. M. Scholtz and D. N. Brems, *Protein Sci.*, 2005, **14**, 1934–1938. Copyright, 2005, Cold Spring Harbor Laboratory Press.

residual structure appears to lead to compensatory loss of native and non-native residual structure causing no net effect on folding.

Thus, when denatured state residual structure involves predominately non-native interactions, the effects on folding appear to be more readily predictable. When these interactions are maintained in the transition state, mutations to remove these interactions primarily affect the unfolding rate leaving the folding rate largely unaffected. When these interactions must be broken in the transition state, the major affect of the mutations will be on the rate of folding. When both native and non-native interactions exist, the effects on folding kinetics are not

 

readily predicable. An example where the denatured state interactions are predominately native like would be an important complement to the existing data.

## Manipulating global stability with the denatured state

Use of the denatured state to modulate the global stability of proteins has a long history. Early approaches focused on manipulating the entropy of the protein main chain in the denatured state. In particular, decreasing the entropy of the denatured state, by introducing disulfide crosslinks[70,134,135] or by using Gly to Ala or Ala to Pro mutations,[136] has been used with some success as a strategy to increase the global stability of proteins. Unfortunately, such methods can also introduce strain in the native state or produce stable compact denatured states leading to unpredictable results.[71,134,137] For example, strain is introduced in folded proteins when non-glycine residues have positive $\phi$ angles due to unfavorable steric clashes between the side chain and the main chain.[137] Since, glycine residues are typically found at such positions, an approach that can reduce the entropy of the denatured state without introducing native state strain is to replace Gly residues with positive $\phi$ values with D-Ala residues. Recent advances in peptide synthesis methods have made this strategy practical and have led to increases in global stability of up to $\sim$2 kcal mol$^{-1}$.[138]

Relative to other methods that affect chain entropy, denatured state histidine–heme loops have the advantage that the histidine which forms the loop can be placed on the protein surface minimizing the impact on the native state. The global stability in a series of iso-1-cytochrome *c* variants correlates quite well with the stability of the loop under denaturing conditions.[72] However, since the histidine–heme interaction stabilizes the denatured state, this type of denatured state interaction decreases global stability.

Studies on stabilizing electrostatic interactions in the denatured state have led to particularly fruitful methods to enhance global stability. Mutation of Lys 12, the primary contributor to the stabilizing non-native electrostatic interactions in NTL9, to a methionine increases global stability by nearly 2 kcal mol$^{-1}$. Measurement of stability as a function of pH as well as the necessary side chain p$K_a$ values, can be applied readily to many proteins. Thus, this approach should be broadly applicable as a means of rationally enhancing protein stability. Recently, this electrostatic method has been combined with the Gly to D-Ala mutational strategy described above producing a hyperstable variant of NTL9 with a melting temperature of 83.1 °C in 6 M urea.[139]

Manipulation of $\Delta C_p$, as mediated by interactions in the denatured state, has also proven useful in increasing the unfolding midpoint temperature of RNase H. The strategy in this case involved making chimeras of thermophilic and mesophilic RNase H and led to an increase in the $T_m$ of the mesophilic protein by 20 °C.[76] It should be noted that the global stability near 298 K in the chimeric protein was similar to the wild type mesophilic protein, but significantly greater at lower or higher temperatures.

Recent progress in our understanding of the thermodynamics of protein denatured states has led to rational strategies for manipulating the global stability of proteins. Stability increases on the order of the largest stabilizations achieved using strategies based solely on optimization of native state interactions are clearly achievable. Native and denatured state strategies for increasing protein stability are now approaching levels of sophistication that a melding of the two approaches might be expected to produce proteins of extraordinary stability.

## Conclusions

The detection of residual structure in protein denatured states has led to a burgeoning of recent effort to characterize the thermodynamic significance of this residual structure. Current data demonstrate that the stability of denatured state residual structure can be up to 4 kcal mol$^{-1}$. Thus, rational manipulation of this structure can lead to substantial effects on the global stability of a protein. Thermodynamic methods are also providing important insights into how factors such as excluded volume, compactness and internal friction of a protein chain affect the early events in protein folding. Studies which correlate the stability of denatured state structure with folding kinetics are also shedding light into how the denatured state impacts the efficiency of protein folding. Thus, protein denatured states are proving to have many interesting and unusual properties that are essential to understanding protein folding and stability.

A number of future directions are evident from the preceding text. A more complete understanding the role of non-native *versus* native like denatured state structure in modulating folding efficiency is essential. While quantitative measurements of the strength of denatured state electrostatic interactions have been made, similar measurements for purely hydrophobic interactions, particularly those modulated by aromatics like tryptophan, are needed. For protein engineers, techniques for combining native and denatured state approaches to protein stabilization to create hyperstable proteins would be a useful next step. The recent progress in our understanding of denatured state thermodynamics provides an excellent foundation for such advances.

## Acknowledgements

The author acknowledges both the NSF and the NIH for long term support of research on protein denatured states, most recently from NIH GM074750-01. The author also thanks the contributors to this work in his laboratory: Lynn Herrmann, Shubhada Godbole, Niels From, Barb Hammack, Chris Smith, Eydiejo (Wandschneider) Kurchan, and Franco Tzul. The author thanks Gary J. Pielak for helpful discussions and the reviewers for their insightful comments.

## References

1 P. L. Privalov and S. J. Gill, *Adv. Protein Chem.*, 1988, **39**, 191–234.
2 K. A. Dill, *Biochemistry*, 1990, **29**, 7133–7155.
3 A. E. Eriksson, W. A. Baase, X.-J. Zhang, D. W. Heinz, M. Blaber, E. P. Bladwin and B. W. Matthews, *Science*, 1992, **255**, 178–183.
4 A. E. Eriksson, W. A. Baase and B. W. Matthews, *J. Mol. Biol.*, 1993, **229**, 747–769.
5 J. B. Holder, A. F. Bennett, J. Chen, D. S. Spencer, M. P. Byrne and W. E. Stites, *Biochemistry*, 2001, **40**, 13998–14003.
6 J. Chen and W. E. Stites, *Biochemistry*, 2001, **40**, 14004–14011.

7 J. Chen and W. E. Stites, *Biochemistry*, 2001, **40**, 14012–14019.
8 J. Chen and W. E. Stites, *Biochemistry*, 2001, **40**, 14280–14289.
9 M. Wang, T. E. Wales and M. C. Fitzgerald, *Proc. Natl. Acad. Sci. U. S. A.*, 2006, **103**, 2600–2604.
10 A. Horovitz, L. Serrano, B. Avron, M. Bycroft and A. R. Fersht, *J. Mol. Biol.*, 1990, **216**, 1031–1044.
11 D. E. Anderson, W. J. Becktel and F. W. Dahlquist, *Biochemistry*, 1990, **29**, 2403–2408.
12 R. Loewenthal, J. Sancho and A. R. Fersht, *J. Mol. Biol.*, 1992, **224**, 759–770.
13 S. S. Strickler, A. V. Gribenko, A. V. Gribenko, T. R. Keiffer, J. Tomlinson, T. Reihle, V. V. Loladze and G. I. Makhatadze, *Biochemistry*, 2006, **45**, 2761–2766.
14 C. M. Dobson, *Nature*, 2003, **426**, 884–890.
15 K. W. Plaxco, K. T. Simons and D. Baker, *J. Mol. Biol.*, 1998, **277**, 985–994.
16 V. Daggett and A. R. Fersht, *Trends Biochem. Sci.*, 2003, **28**, 18–25.
17 C. Levinthal, *J. Chim. Phys. Phys.-Chim. Biol.*, 1968, **65**, 44–45.
18 K. A. Dill and H. S. Chan, *Nat. Struct. Biol.*, **4**, 10–19.
19 A. R. Fersht, *Structure and Mechanism in Protein Science*, W. H. Freeman and Co., New York, Chapter 19.
20 P. S. Kim and R. L. Baldwin, *Annu. Rev. Biochem.*, 1990, **59**, 631–660.
21 Y. Bai, T. R. Sosnick, L. Mayne and S. W. Englander, *Science*, 1995, **269**, 192–197.
22 R. T. Baldwin, *J. Biomol. NMR*, 1995, **4**, 103–109.
23 P. G. Wolynes, *Philos. Trans. R. Soc. London, Ser. A*, 2005, **363**, 453–467.
24 S. E. Jackson, *Fold. Des.*, 1998, **3**, R81–R91.
25 A. R. Fersht, *Proc. Natl. Acad. Sci. U. S. A.*, 2000, **97**, 1525–1529.
26 D. Neri, M. Billeter, G. Wider and K. Wuthrich, *Science*, 1992, **257**, 1559–1563.
27 H. J. Dyson and P. E. Wright, *Chem. Rev.*, 2004, **104**, 3607–3622.
28 J. R. Gillespie and D. Shortle, *J. Mol. Biol.*, 1997, **268**, 170–184.
29 D. Shortle and M. S. Ackerman, *Science*, 2001, **293**, 487–489.
30 O. Zhang and J. D. Forman-Kay, *Biochemistry*, 1997, **36**, 3959–3970.
31 Y.-K. Mok, C. M. Kay, L. E. Kay and J. Forman-Kay, *J. Mol. Biol.*, 1999, **289**, 619–638.
32 J. Klein-Seetharaman, M. Oikawa, S. B. Grimshaw, J. Wirmer, E. Duchardt, T. Ueda, T. Imoto, L. J. Smith, C. M. Dobson and H. Schwalbe, *Science*, 2002, **295**, 1719–1722.
33 P. A. Evans, K. D. Topping, D. N. Woolfson and C. M. Dobson, *Proteins: Struct., Funct. Genet.*, 1991, **9**, 248–266.
34 H. Schwalbe, K. M. Fiebig, M. Buck, J. A. Jones, S. B. Grimshaw, A. Spencer, S. J. Glaser, L. J. Smith and C. M. Dobson, *Biochemistry*, 1997, **36**, 8977–8991.
35 K. A. Crowhurst and J. D. Forman-Kay, *Biochemistry*, 2003, **42**, 8687–8695.
36 J. Clarke, A. M. Hounslow, C. J. Bond, A. R. Fersht and V. Daggett, *Protein Sci.*, 2000, **9**, 2394–2404.
37 K.-B. Wong, J. Clarke, C. J. Bond, J. L. Neira, S. M. V. Freund, A. R. Fersht and V. Daggett, *J. Mol. Biol.*, 2000, **296**, 1257–1282.
38 S. L. Kazmirski, K.-B. Wong, S. M. V. Freund, Y.-J. Tan, A. R. Fersht and V. Daggett, *Proc. Natl. Acad. Sci. U. S. A.*, 2001, **98**, 4349–4354.
39 W.-Y. Choy and J. D. Forman-Kay, *J. Mol. Biol.*, 2001, **308**, 1011–1032.
40 *Unfolded Proteins*, ed. G. D. Rose, *Advances in Protein Chemistry*, Academic Press, New York, 2002, vol. 62.
41 C. Tanford, *Adv. Protein Chem.*, 1968, **23**, 121–282.
42 C. Tanford, K. Kawahara and S. Lapanje, *J. Am. Chem. Soc.*, 1967, **89**, 729–736.
43 P. J. Fleming and G. D. Rose, *Protein Folding Handbook, Part I*, ed. J. Buchner and T. Kiefhaber, Wiley-VCH, Weinheim, 2005, pp. 710–736.
44 D. K. Wilkins, S. B. Grimshaw, V. Receveur, C. M. Dobson, J. A. Jones and L. J. Smith, *Biochemistry*, 1999, **38**, 16424–16431.
45 J. E. Kohn, I. S. Millet, J. Jacob, B. Zagrovic, T. M. Dillon, N. Cingel, R. S. Dothager, S. Seifert, P. Thiyagarajan, T. R. Sosnick, M. Z. Hasan, V. J. Pande, I. Ruczinski, S. Doniach and K. W. Plaxco, *Proc. Natl. Acad. Sci. U. S. A.*, 2004, **101**, 12491–12496.
46 M. L. Tiffany and S. Krimm, *Biopolymers*, 1972, **11**, 2309–2316.
47 M. L. Tiffany and S. Krimm, *Biopolymers*, 1973, **12**, 575–587.
48 R. W. Woody, *Adv. Biophys. Chem.*, 1992, **2**, 37–79.
49 Z. Shi, K. Chen, Z. Liu and N. R. Kallenbach, *Chem. Rev.*, 2006, **106**, 1877–1897.
50 K. C. Aune, A. Salahuddin, M. H. Zalengo and C. Tanford, *J. Biol. Chem.*, 1967, **242**, 4486–4489.
51 T. Y. Tsong, *J. Biol. Chem.*, 1974, **249**, 1988–1990.
52 T. Y. Tsong, *Biochemistry*, 1975, **14**, 1542–1547.
53 D. Shortle and A. K. Meeker, *Proteins: Struct., Funct. Genet.*, 1986, **1**, 81–89.
54 D. Shortle, *Adv. Protein Chem.*, 1995, **46**, 217–247.
55 J. A. Schellman, *Biopolymers*, 1978, **17**, 1305–1322.
56 J. K. Myers, C. N. Pace and J. M. Scholtz, *Protein Sci.*, 1995, **4**, 2138–2148.
57 S. M. Green and D. Shortle, *Biochemistry*, 1993, **32**, 10131–10139.
58 E. K. Pletneva, H. B. Gray and J. R. Winkler, *J. Mol. Biol.*, 2005, **345**, 855–867.
59 P. Chuga, H. J. Sage and T. G. Oas, *Protein Sci.*, 2006, **15**, 533–542.
60 A. A. Pakula and R. T. Sauer, *Nature*, 1990, **344**, 363–364.
61 A. Tamura and J. M. Sturtevant, *J. Mol. Biol.*, 1995, **249**, 646–653.
62 B. E. Bowler, K. May, T. Zaragoza, P. York, A. Dong and W. S. Caughey, *Biochemistry*, 1993, **32**, 183–190.
63 L. Herrmann, B. E. Bowler, A. Dong and W. S. Caughey, *Biochemistry*, 1995, **34**, 3040–3047.
64 V. V. Filimonov and V. V. Rogov, *J. Mol. Biol.*, 1996, **255**, 767–777.
65 G. R. Grimsley, K. L. Shaw, L. R. Fee, R. W. Alston, B. M. Huyghes-Despointes, R. L. Thurkill, J. M. Scholtz and C. N. Pace, *Protein Sci.*, 1999, **8**, 1843–1849.
66 G. Saab-Rincón, C. L. Froebe and C. R. Matthews, *Biochemistry*, 1993, **32**, 13981–13990.
67 G. Saab-Rincón, C. L. Froebe and C. R. Matthews, *Biochemistry*, 1996, **35**, 1988–1994.
68 C. N. Pace, *CRC Crit. Rev. Biochem.*, 1975, **3**, 1–43.
69 S. Godbole, A. Dong, K. Garbin and B. E. Bowler, *Biochemistry*, 1997, **36**, 119–126.
70 C. N. Pace, G. R. Grimsley, J. A. Thomson and B. J. Barnett, *J. Biol. Chem.*, 1988, **263**, 11820–11825.
71 S. J. Betz and G. J. Pielak, *Biochemistry*, 1992, **31**, 12337–12344.
72 E. Wandschneider, B. N. Hammack and B. E. Bowler, *Biochemistry*, 2003, **42**, 10659–10666.
73 I. V. Baskakov and D. W. Bolen, *Biochemistry*, 1998, **37**, 18010–18017.
74 D. Shortle and A. K. Meeker, *Biochemistry*, 1989, **28**, 936–944.
75 J. Wrabl and D. Shortle, *Nat. Struct. Biol.*, 1999, **6**, 876–883.
76 S. Robic, J. M. Berger and S. Marqusee, *Protein Sci.*, 2002, **11**, 381–389.
77 M. Guzman-Casado, A. Parody-Morreale, S. Robic, S. Marqusee and J. M. Sanchez-Ruiz, *J. Mol. Biol.*, 2003, **329**, 731–743.
78 S. Robic, M. Guzman-Casado, S. Marqusee and J. M. Sanchez-Ruiz, *Proc. Natl. Acad. Sci. U. S. A.*, 2003, **100**, 11345–11349.
79 D. Wildes and S. Marqusee, *Methods Enzymol.*, 2004, **380**, 328–349.
80 D. Wildes, L. M. Anderson, A. Sabogal and S. Marqusee, *Protein Sci.*, 2006, **15**, 1769–1779.
81 M.-F. Jeng and S. W. Englander, *J. Mol. Biol.*, 1991, **221**, 1045–1061.
82 J. L. Marmorino, D. S. Auld, S. F. Betz, D. F. Doyle, G. B. Young and G. J. Pielak, *Protein Sci.*, 1993, **2**, 1966–1974.
83 L. Swint-Kruse and A. D. Robertson, *Biochemistry*, 1996, **35**, 171–180.
84 J. L. Neira, P. Sevilla, M. Menéndez, M. Bruix and M. Rico, *J. Mol. Biol.*, 1999, **285**, 627–643.
85 B. M. P. Huyghues-Despointes, J. M. Scholtz and C. N. Pace, *Nat. Struct. Biol.*, 1999, **6**, 910–912.
86 V. P. Grantcharova and D. B. Baker, *Biochemistry*, 1997, **36**, 15685–15692.
87 M. Sadqi, S. Casares, O. López-Mayorga, J. C. Martinez and F. Conejero-Lara, *FEBS Lett.*, 2002, **514**, 295–299.


 

88 N. M. Nicholson, H. Mo, S. B. Prusiner, F. E. Cohen and S. Marqusee, *J. Mol. Biol.*, 2002, **316**, 807–815.
89 N. Bhutani and J. B. Udgaonkar, *Protein Sci.*, 2003, **12**, 1719–1731.
90 J. P. Schmittschmitt and J. M. Scholtz, *Biochemistry*, 2004, **43**, 1360–1368.
91 C. N. Pace, R. W. Alston and K. L. Shaw, *Protein Sci.*, 2000, **9**, 1395–1398.
92 C. N. Pace, D. V. Laurents and J. A. Thomson, *Biochemistry*, 1990, **29**, 2564–2572.
93 C. N. Pace, D. V. Laurents and R. E. Erickson, *Biochemistry*, 1992, **31**, 2728–2734.
94 S. T. Whitten and B. Garcia-Moreno, *Biochemistry*, 2000, **39**, 14292–14304.
95 Y. Li, J.-C. Horng and D. P. Raleigh, *Biochemistry*, 2006, **45**, 8499–8506.
96 B. Kuhlman, D. L. Luisi, P. Young and D. P. Raleigh, *Biochemistry*, 1999, **38**, 4896–4903.
97 J.-H. Cho, S. Sato and D. P. Raleigh, *J. Mol. Biol.*, 2004, **338**, 827–837.
98 J.-H. Cho and D. P. Raleigh, *J. Mol. Biol.*, 2005, **353**, 174–185.
99 M. Oliveberg, S. Vuilleumier and A. R. Fersht, *Biochemistry*, 1994, **33**, 8826–8832.
100 M. Oliveberg, V. L. Arcus and A. R. Fersht, *Biochemistry*, 1995, **34**, 9424–9433.
101 Y. J. Tan, M. Oliveberg, B. Davis and A. R. Fersht, *J. Mol. Biol.*, 1995, **254**, 980–992.
102 L. Swint-Kruse and A. D. Robertson, *Biochemistry*, 1995, **34**, 4724–4732.
103 J.-C. Horng, J.-H. Cho and D. P. Raleigh, *J. Mol. Biol.*, 2005, **345**, 163–173.
104 M. Tollinger, J. D. Forman-Kay and L. E. Kay, *J. Am. Chem. Soc.*, 2002, **124**, 5714–5717.
105 M. Tollinger, K. A. Crowhurst, L. E. Kay and J. D. Forman-Kay, *Proc. Natl. Acad. Sci. U. S. A.*, 2003, **100**, 4545–4550.
106 B. Fierz and T. Kiefhaber, *Protein Folding Handbook, Part I*, ed. J. Buchner and T. Kiefhaber, Wiley-VCH, Weinheim, 2005, pp. 809–855.
107 J. Kubelka, M. Buscaglia, J. Hofrichter and W. A. Eaton, *NATO Science Series, Series I: Life and Behavioral Sciences, Structure, Dynamics and Function of Biological Macromolecules and Assemblies*, ed. J. Puglisi, IOS Press, Amsterdam, **vol. 364**, 2005, pp. 1–10.
108 J. R. Winkler, *Curr. Opin. Chem. Biol.*, 2004, **8**, 169–174.
109 S. Godbole and B. E. Bowler, *J. Mol. Biol.*, 1997, **268**, 816–821.
110 S. GodboleB. Hammack and B. E. Bowler, *J. Mol. Biol.*, 2000, **296**, 217–228.
111 B. N. Hammack, C. R. Smith and B. E. Bowler, *J. Mol. Biol.*, 2001, **311**, 1091–1104.
112 H. S. Chan and K. A. Dill, *Annu. Rev. Biophys. Biophys. Chem.*, 1990, **20**, 447–490.
113 H. S. Chan and K. A. Dill, *J. Chem. Phys.*, 1990, **92**, 3118–3138.
114 S. Redner, *J. Phys. A: Math. Gen.*, 1980, **12**, 3525–3541.
115 S. V. Kutznetsov, Y. Shen, A. S. Benight and A. Ansari, *Biophys. J.*, 2001, **81**, 2864–2875.
116 Y. Shen, S. V. Kuznetsov and A. Ansari, *J. Phys. Chem. B*, 2001, **105**, 12202–12211.
117 E. Wandschneider and B. E. Bowler, *J. Mol. Biol.*, 2004, **339**, 185–197.
118 E. Kurchan, H. Roder and B. E. Bowler, *J. Mol. Biol.*, 2005, **353**, 730–743.
119 S. Hagen, L. Qui and S. A. Pabit, *J. Phys.: Condens. Matter*, 2005, **17**, S1503–S1514.
120 C. R. Smith, N. Mateljevic and B. E. Bowler, *Biochemistry*, 2002, **41**, 10173–10181.
121 J. G. Lyubovitsky, H. B. Gray and J. R. Winkler, *J. Am. Chem. Soc.*, 2002, **124**, 5481–5485.
122 F. A. Tezcan, W. M. Findley, B. R. Crane, S. A. Ross, J. G. Lyubovitsky, H. B. Gray and J. R. Winkler, *Proc. Natl. Acad. Sci. U. S. A.*, 2002, **99**, 8626–8630.
123 J. C. Lee, I.-J. Chang, H. B. Gray and J. R. Winkler, *J. Mol. Biol.*, 2002, **320**, 159–164.
124 T. R. Sosnick, L. Mayne, R. Hiller and S. W. Englander, *Nat. Struct. Biol.*, 1994, **1**, 149–156.
125 S.-R. Yeh, S. Takahashi, B. Fen and D. L. Rousseau, *Nat. Struct. Biol.*, 1997, **4**, 51–56.
126 W. Colón, L. P. Wakem, F. Sherman and H. Roder, *Biochemistry*, 1997, **41**, 12535–12541.
127 M. Panda, M. G. Benavides-Garcia, M. M. Pierce and B. T. Nall, *Protein Sci.*, 2000, **9**, 536–543.
128 B. Hammack, S. Godbole and B. E. Bowler, *J. Mol. Biol.*, 1998, **275**, 719–724.
129 J. N. Rumbley, L. Hoang and S. W. Englander, *Biochemistry*, 2002, **41**, 13894–13901.
130 J. M. Trefethen, C. N. Pace, J. M. Scholtz and D. N. Brems, *Protein Sci.*, 2005, **14**, 1934–1938.
131 M. Karplus and D. L. Weaver, *Protein Sci.*, 1994, **3**, 650–668.
132 Y. Tang, D. J. Rigotti, R. Fairman and D. P. Raleigh, *Biochemistry*, 2004, **43**, 3264–3272.
133 S. H. Brewer, D. M. Vu, Y. Tang, Y. Ling, S. Franzen, D. P. Raleigh and R. B. Dyer, *Proc. Natl. Acad. Sci. U. S. A.*, 2005, **102**, 16662–16667.
134 M. Matsumara and B. W. Matthews, *Meth. Enzymol.*, 1991, **202**, 336–357.
135 S. F. Betz, *Protein Sci.*, 1993, **2**, 1551–1558.
136 B. W. Matthews, H. Nicholson and W. J. Becktel, *Proc. Natl. Acad. Sci. U. S. A.*, 1987, **84**, 6663–6667.
137 W. E. Stites, A. K. Meeker and D. Shortle, *J. Mol. Biol.*, 1994, **235**, 27–32.
138 B. Anil, B. Song, Y. Tang and D. P. Raleigh, *J. Am. Chem. Soc.*, 2004, **126**, 13194–13195.
139 B. Anil, R. Craig-Shapiro and D. P. Raleigh, *J. Am. Chem. Soc.*, 2006, **128**, 3144–3145.
140 J.-L. Fauchère and V. Pliška, *Eur. J. Med. Chem.*, 1983, **18**, 369–375.